Solid Freeform Fabrication 2024: Proceedings of the 35th Annual International Solid Freeform Fabrication Symposium – An Additive Manufacturing Conference
Reviewed Paper

4D Printed Actuation with Spatially-Varying Lattices

Katia L. Delgado Ramos[1], Ana Paola Aranzola[1], Ijaz Akbar[2],
Aaron Cervantes[1], Ana C. Martínez[1], Alexis Maurel[1], Eric MacDonald [1,3],
Alejandra G. Castellanos[2], Mohamed El Mansori[2], David A. Roberson[1,*]

[1]The University of Texas at El Paso, TX USA 79968

[2]Arts et Métiers ParisTech (ENSAM), Aix-en-Provence, FRANCE 13617

[3] Manufacturing Science Division, Oak Ridge National Laboratory, TN USA 37830

* Corresponding author: droberson@utep.edu

Abstract

Creating 3D printed structures from materials with shape memory properties allows these structures to change form, modifying configuration or function over time in response to external stimuli such as temperature, light, electrical current, etc. This area of additive manufacturing has come to be known as 4D printing. A variety of geometries have been previously explored in the context of 4D printing, including foldable surfaces (e.g. Origami), lattices, and bio-inspired shapes. However, with advances in solid modeling software tools, more sophisticated spatially-varying lattices are now easily generated to further optimize the mechanical performance and functionality of a 4D printed structure. In this work, complex lattices are created to bend at specific locations with intentionally-reduced stiffness and improved compliance based on locally-reduced strut dimensions. By experimentally demonstrating more complex geometries in the study of 4D printing, new applications can be considered that were not previously possible, with tailored performance allowing for balancing between weight and actuation.

Keywords: Additive Manufacturing, Spatially-Varying Lattices, 4D Printing, Actuation, Shape memory polymers

1. Introduction

4D printing has been adopted as an innovative technology, providing advancement beyond the traditional benefits of 3D printing, which is capable of fabricating conventional static structures of complex geometries. 4D printing adds the fourth dimension, providing the ability of a printed structure to change shape or react to different stimuli applied over time in comparison to the traditional load-bearing structures created with 3D printing [1,2]. The key enabler of this aspect of additive manufacturing (AM) is the integration of shape memory materials. In other words, 4D printing combines 3D printing with advanced materials that reversibly metamorphosize with the application of a stimulus [3]. Shape memory polymers (SMP)s allow the holding of a temporary shape, and then the recovery of an initial "programmed" shape by applying an external stimulus [4–8], such as light [9,10], heat [11,12], moisture [13], pH [14], electricity [15], etc. The main characteristic of SMPs is the ability to recover their original shape due to viscoelastic flow [16,17]. There are two main mechanisms that characterize the shape memory function in polymers: 1) dual

component, where the temporary shape is held by a physically soft material phase and the permanent shape is “remembered” by a physically hard material phase; and 2) dual state, where the temporary shape is held by soft crosslinks such as hydrogen bonding or chain entanglement and the permanent shape is preserved by strong crosslinks such as covalent bonds [18].

SMPs when compared to metals or ceramics have advantages in that many are biodegradable, biocompatible [19], provide reduced material cost, possess an inherent lower density, and improved mechanical properties [20–22]. SMPs have been applied in distinct fields such as the aerospace and biomedical industries [23–26], and one popular example of commercial feedstock that exhibits shape memory properties [27] is polylactic acid (PLA) - a common feedstock in desktop 3D printing due to the low cost and ease of printing [28] where Ingeo 4043D (Natureworks, Minnetonka MN, USA) is a common grade used by filament manufactures and Grade 3D870 is commonly marketed as PLA+ [29]. The shape memory properties of PLA are well-characterized and they are driven by the dual state mechanism. Furthermore, PLA is bio-based and provides biodegradability and biocompatibility - a focal point of industrial research in recent decades [18,30,31].

The integration of metamaterial design practices with 3D printing allows for the creation of structures tailored to achieve different and more profound mechanical properties as compared to traditional structural design [32,33]. A mechanical or structural metamaterial is a kind of metamaterial with a unique mechanical property based on the structure more than the inherent mechanical properties of the material [34]. These unusual properties obtained are the result of the specific design and are often can only be fabricated with the use of additive manufacturing [35].

One example of an unusual property include negative Poisson’s ratio which occurs through applying a force that can contract or expand in multiple directions, demonstrating how the design can provide unintuitive behavior [36], also exhibiting negative elasticity and negative compressibility [37]. Moreover, if the metamaterials are created by smart materials such as shape memory polymers, more pronounced and counter-intuitive results such as environmental adaptability and large deformation capacity [38] can now be achieved. Smart structures can respond to changes in the environment and adapt or provide other functionality [39,40].

Another development associated with 4D printing is the enabling of the creation of adaptable properties in lattice structures [41] leveraging the unique aspects of the lattices and the ability to tune mechanical performance and provide a balance between strength, weight and stiffness. Additionally, materials with shape memory properties have the ability to adapt to a variety of spatial and temporal shapes [42]. It is paramount to use mathematical modeling to simulate multi-material 4D printing in order to guide the computer-aided design (CAD), and orientation as well as the calculation of the expansion and contraction rates of the stimulus response to obtain an effective reversible form [43].

The present work explores the benefits of spatially-varying lattices in the context of 4D printing. By leveraging recently available geometry-generating CAD tools that enable lattice designs in which the unit cell size remains the same, but with a modulation in strut size, it is hypothesized that 4D printing performance can be improved. Furthermore, with the aid of computer-aided modeling, complex design spaces can be readily explored. Digital image correlation (DIC) of two of the geometries was to demonstrate the utility of simulations to guide design. Based on a combination of geometry and materials, an experiment was performed with programmable lattice structures with different density fields with the intention of bending at targeted angles of 30°, 45°, 60° and 90°. Repeatability, actuation endurance, and mechanical properties along with inspection with DIC and SEM were completed.

2. Materials and Methods

Lattices were designed with a range of compliance using nTopology. The designs were printed with PLA, which has inherent shape memory properties. The deformation and recovery temperatures have been well-documented in literature. Previous work by our group involving PLA has found characterization by way of dynamic mechanical analysis (DMA) to provide the determination of the critical deformation and recovery temperatures at 60 ℃ (the glassy onset temperature) and 70 °C (the temperature at which the max tan δ occurs) [44]. The parts were deformed after first heating them in a horizontal air flow oven (VWR International, PA, USA). The specimens were then recovered in heated water at the recovery temperature where the recovery process was recorded and the video processed using digital image correlation.

2.1 Lattice design

The spatially varying structures were designed in the CAD software, nTopology (nTopology, New York, USA). For this study, a cylindrical BCC lattice measuring 90 mm in length and 20 mm in diameter was created, mimicking the dimensions of a human finger to explore applications in robotic actuation. Additionally, this architecture allowed thermoplastic extrusion 3D printing without the use of support structures. To achieve a cosine wave function within a cylindrical 90 mm long and 20 mm diameter BCC lattice (approximating a human finger targeting robotic actuation applications), a scalar field with the shape of a box was remapped in the x-axis. The box scalar field must have greater dimensions than the cylinder in the three axes and remapping formulas should be as follows to achieve a single cosine period for a cylinder:

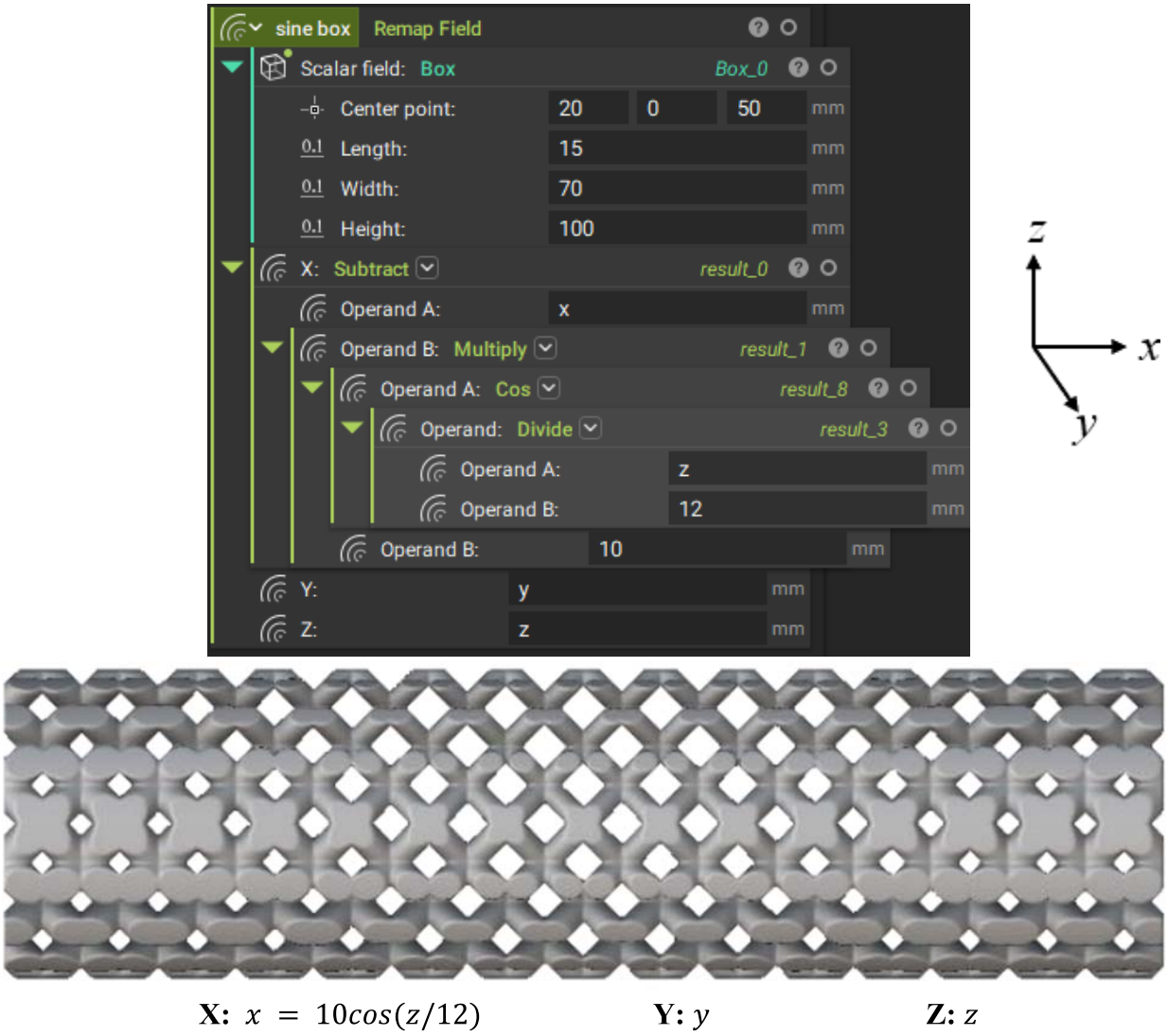

Figure 1: nTopology code block (top) to create the remapped field to create a modulation of the BCC lattice with spatially varying thickness in the x-axis which follows the shape of the cosine wave function, x =10cos(z/12).

Four spatially-varying cylinders were designed by altering a cosine equation to achieve four different spatially-varying density fields allowing for a range of bending compliances in the X axis to permit shape memory programming with different angle extents. By correctly programming the density field, the amount of bending could be tailored for a specific shape memory application such as soft robotic actuation.

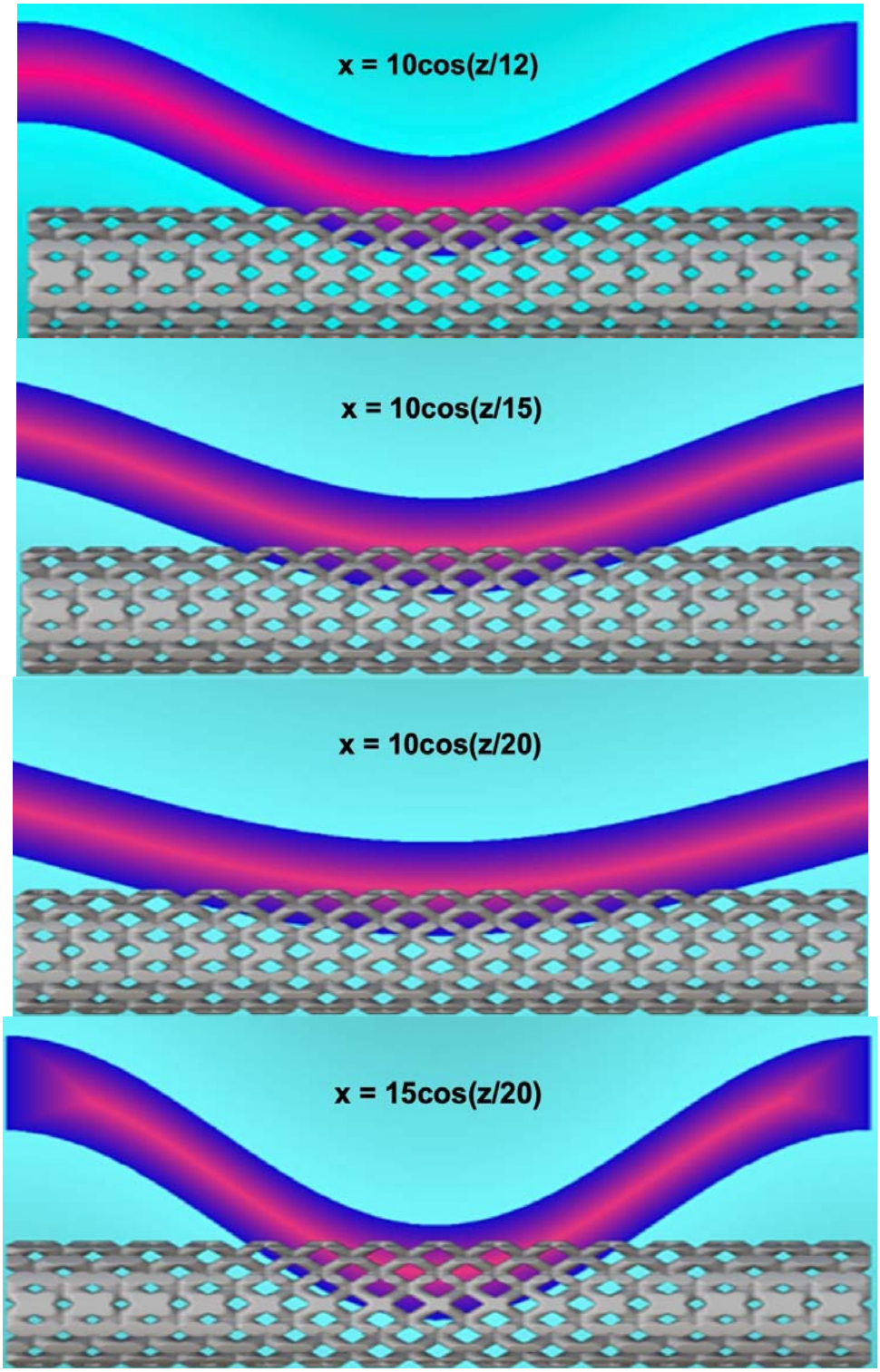

Figure 2: Four spatially-varying lattice architectures with different bending compliances.

2.2 4D Printing Process, Material, and Programming

The workflow for the experimental design and fabrication is shown in **Figure 3**. The material used for this paper project is from MatterHackers (White PRO Series PLA Filament, MatterHackers, Valencia, CA, USA) with a diameter of 1.75 mm. All the specimens were printed on an FFF machine Original Prusa MINI+ Semi-assembled 3D Printer. The parameters and the temperature of the spatially varying lattice printed were configured by a slicer program with a bed temperature of 60 °C, and nozzle temperature of 215 °C, using a nozzle diameter of 0.4 mm.

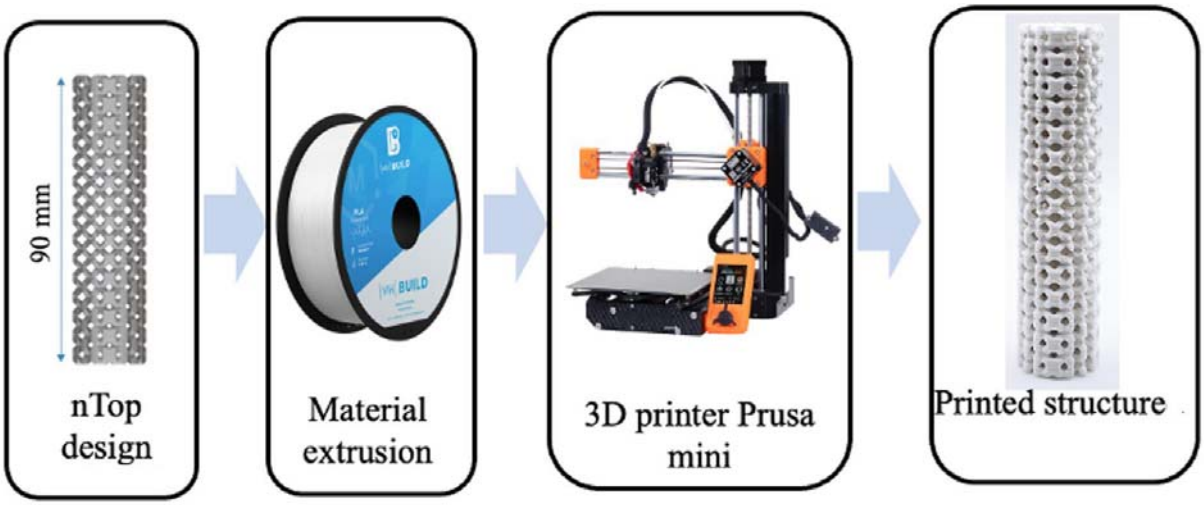

Figure 3: Printing design process with standard commercial PLA material.

2.3 Actuation Evaluation and Digital Image Correlation (DIC)

One sample from each of the four lattice structures underwent DIC to measure their deformation and recovery time. First, a speckle pattern was applied to the surface of the lattice structures, followed by heating them uniformly in an oven above the glass transition temperature (T_g) of PLA to establish a temporary form. Then, they were left to cool down to room temperature. Once they reached room temperature, the deformed lattices were placed in a container with water that was heated to a temperature of 70 °C. Images of the deforming specimen due to the water temperature were captured using a Google Pixel 7 camera, which has a 50 megapixel (MP) resolution at a rate of 30 frames per second. Utilizing py2DIC [45], an open-source local 2D DIC software developed by the Geodesy and Geomatics Division of Sapienza University of Rome, the 2D displacement was estimated from the image set. Notably, the DIC measurements provided comprehensive field measurements. The recovery process recorded through DIC can be seen in

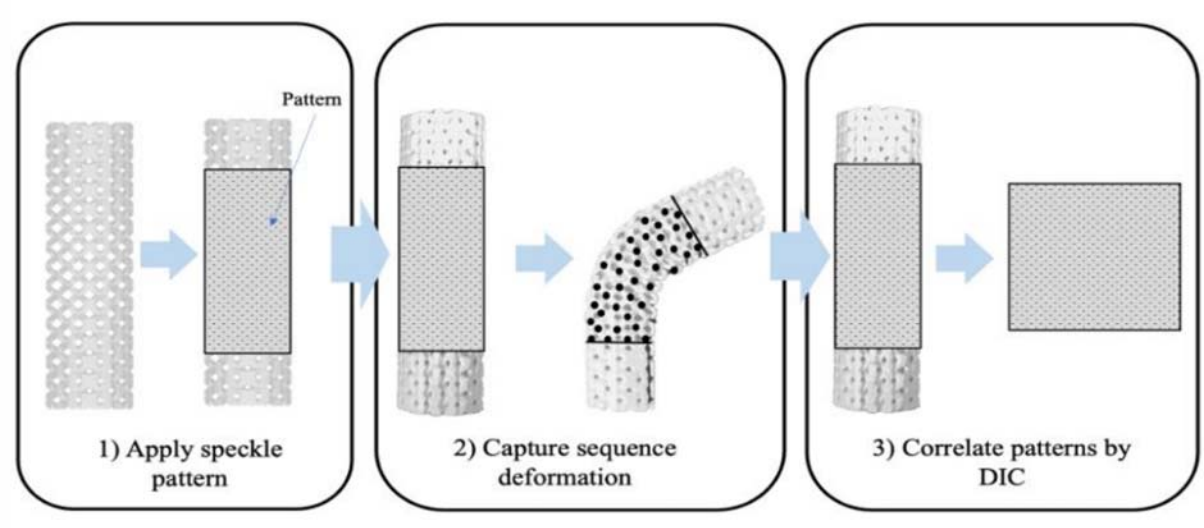

Figure 4: Process of recovery structure by Digital Image Correlation (DIC).

2.4 SEM Characterization

SEM characterization of the surfaces was carried out on a Hitachi (Hitachi America, Ltd., New York USA) SU3500 scanning electron microscope (SEM) operating with an acceleration voltage of 15 kV, and using a backscattered electron (BSE) detector. To mitigate the effects of electron charging, the instrument was operated in variable pressure mode at a pressure of 90 Pa. We chose to use this instrument to allow for precise measurement of the cell dimension and to observe artifacts associated with the AM process. This technique also allowed for the analysis of the wavelength through the observation of the central joint of the piece, the size of the struts as well as the quality of the printing process.

3. Results and Discussion

3.1 Printing Results and SEM evaluation

As illustrated in **Figure 5**, the intricate details of the lattice structures were printed reasonably well with the Prusa low-cost desktop printer. However, these details were at the resolution limit of the printer, suggesting that further reductions in minimum feature size may not be achievable. **Figure 6** illustrates how the struts were printed with obvious layers but with reasonable stair stepping in order to accurately realize the intended geometry. Moreover, the density variation is evaluated by measuring the size of two arbitrarily chosen voids, one in the middle in the sparse density region included a hole of 1.242 mm width as dictated by the dimensional measurement. Farther below in the structure, in a section with higher density, the void had a smaller width of 1.027 mm demonstrating the increased density and stiffness.

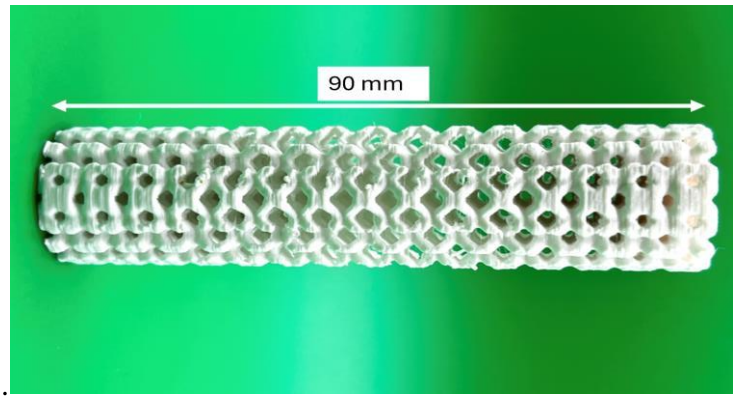

Figure 5: An example of a printed result with spatial density following the x=10cos(z/20) field.

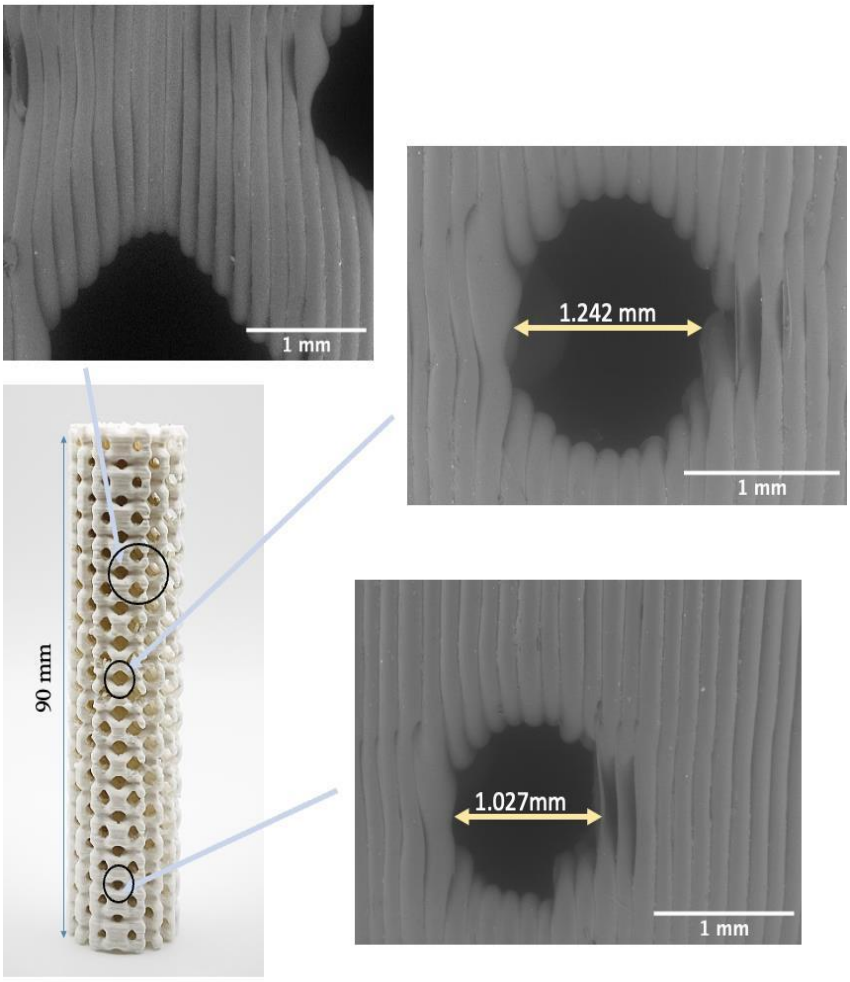

Figure 6: SEM image of the central joint of the structure.

3.2 Digital Image Correlation Results

The DIC measurements allowed us to measure the displacement field of the lattice structures. The graph in **Figure 7** identifies that the maximum angle was achieved for the x = 10cos(z/12) geometry, which showed an angle of 61° at an interval of 24.9 seconds. For the x = 15cos(z/12), the maximum angle observed was 59° at 19.6 seconds. The x = 10cos(z/15) geometry yielded an angle of 52° at 21.85 seconds. However, the minimum angle achieved was exhibited by the x = 10cos(z/20) geometry with an angle of 37° at 19.7 seconds.

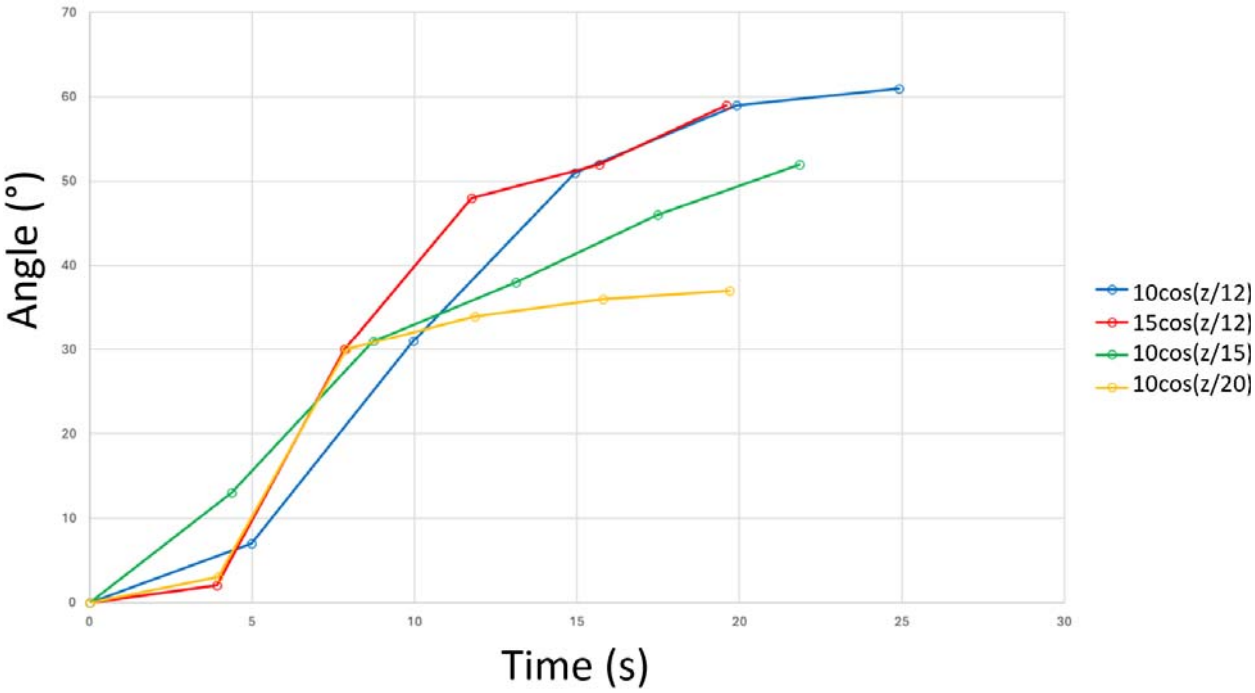

Figure 7: Digital image correlation for all four lattice designs.

The DIC enabled the identification of discrete levels of deformation on the lattice structure surfaces. In this method, the strain value is a structural strain. From the DIC images **Figure 8** and **Figure 9**, it is possible to observe an initial stage of deformation on the top of each image and a recovered form at the bottom right showing the release of the compression. The lattice structure shows a maximum shear strain angle on x = 10cos(z/12) at 61°, when the specimen was under compression. The DIC showed the maximum displacement of 26.3 mm. **Figure 10** illustrates one example of a lattice stricture after programming (bent at approximately 90°), and subsequently, after recovery when placed in warm water as a thermal stimulus.

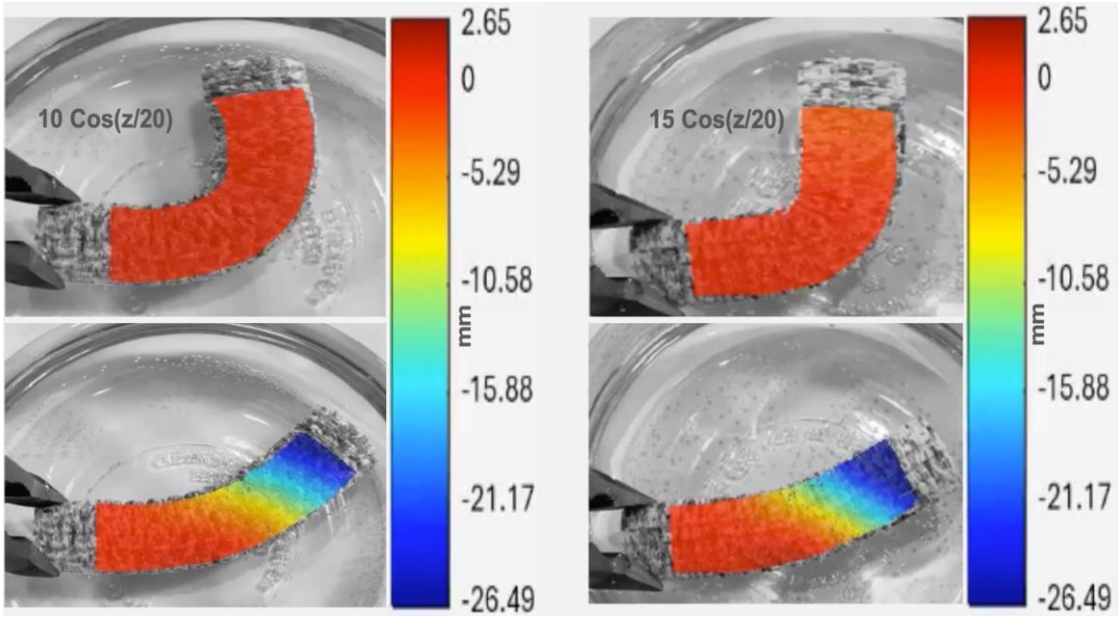

Figure 8: Schematic of digital image correlation of x = 10cos(z/20) (left) and x = 15cos(z/20) (right). Top images display the initial stage of deformation, and bottom images display a recovered form showing the release of the compression.

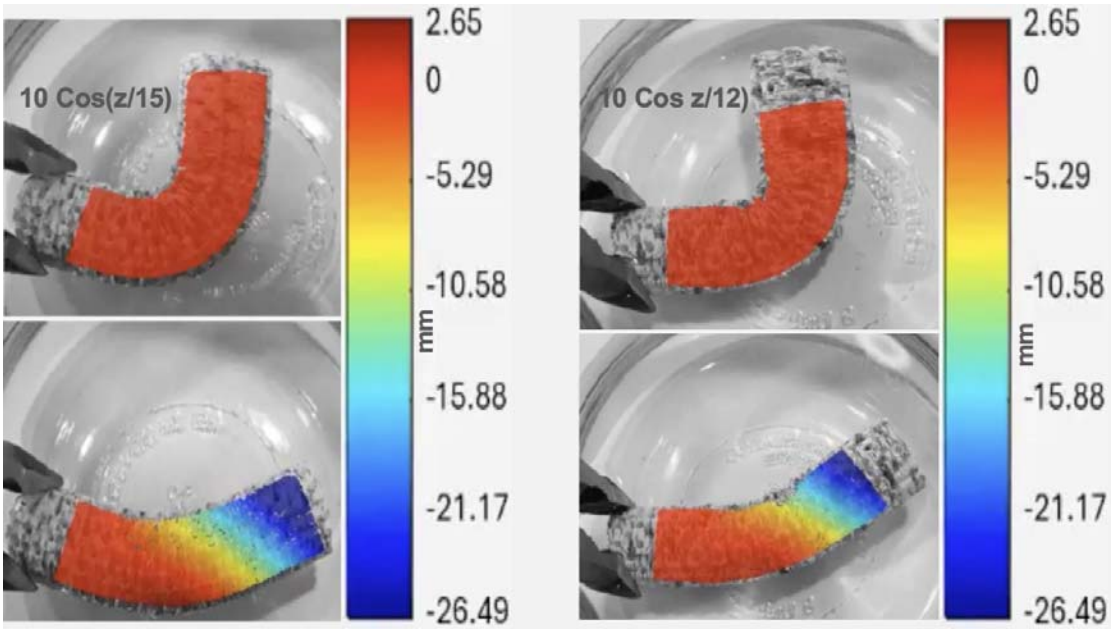

Figure 9: Schematic of digital image correlation of x = 10cos(z/15) (left) and x = 10cos(z/12) (right). Top images display the initial stage of deformation, and bottom images display a recovered form showing the release of the compression.

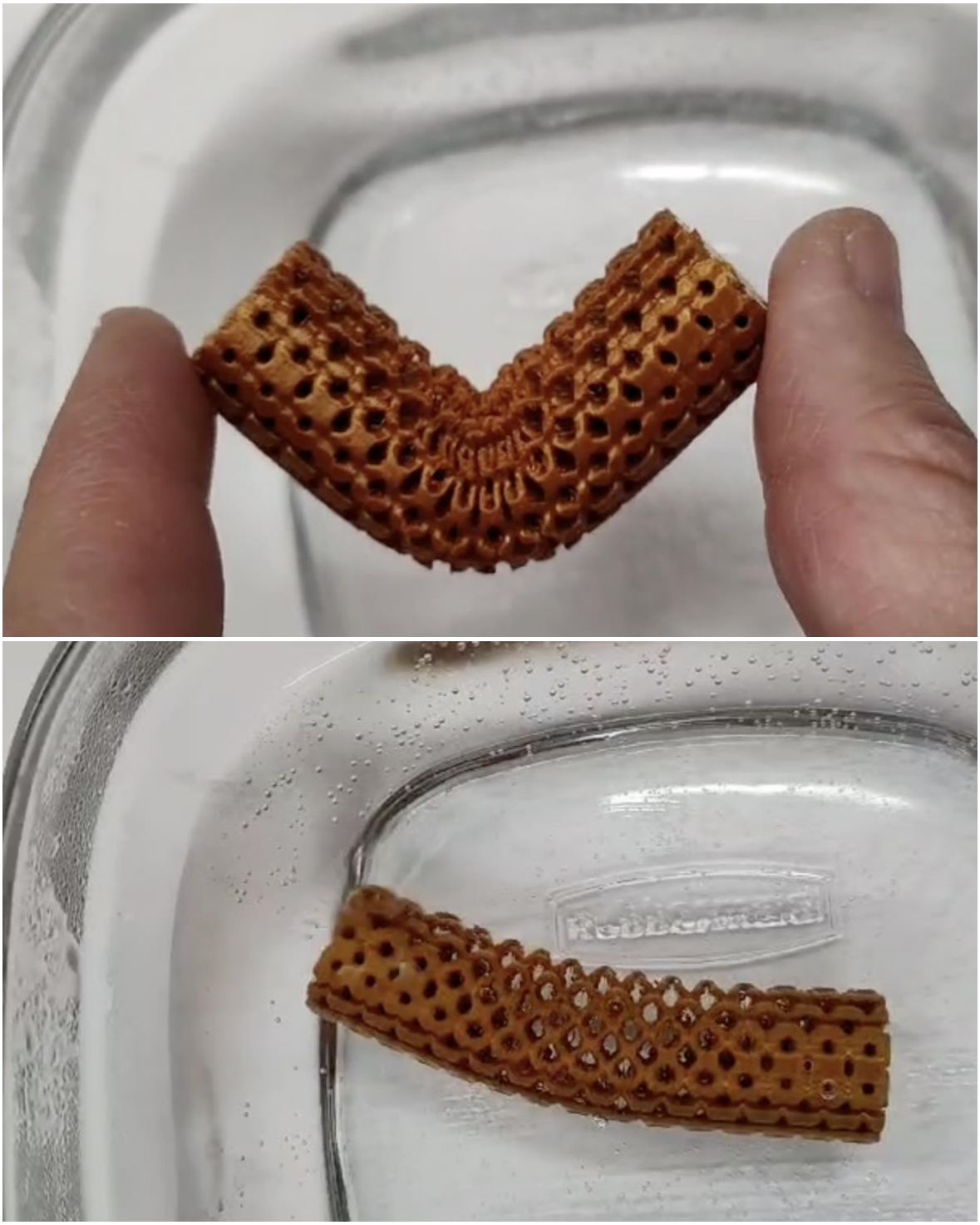

Figure 10: x = 10cos(z/12) in the deformed condition (top) and after almost-complete recovery (bottom) demonstrating the utility of spatially-varying lattices to achieve optimal compliance in shape memory applications.

4.0 Conclusions and Future Work

The combination of spatially variant design was successfully integrated with the methodology of 4D printing, a combination of AM and shape memory materials. The spatially variant structures allowed for the design of actuating beams with a discrete range of motion. This design principle can be applied to the development of soft robotics where discrete range of motion can be used to create self-ambulatory devices and other functional components such as grippers. Moreover, the integration of spatially variant structures could also benefit the design of self-deployable structures.

The DIC analysis was accurate and reproducible with water at different temperatures applied to the lattice structures. The graphs illustrate variations corresponding to the alternation of struts and nodes. The printing quality was evaluated and denoted by SEM. In addition, the viscoelastic behavior and above the T_g helped to intensify the chain mobility of the structure which allowed to obtain a shape memory behavior. The correlation length is related to the design orientation of the wavelength which can be identified from the digital image correlation.

Future work will entail the shape memory programming and recovery of such artifact lattice structure will be discussed through detailed numerical and experimental findings. The following physics-based relationships such as programming strain (ε_{prog}), internal/irrecoverable strains (ε_{irr}), hermal strains and the material properties (ratio of hard to soft segments of the selected SMP) will be considered in calculating and validating the shape memory actions [46] :

$$R_r = \frac{\varepsilon_{rec}}{\varepsilon_{prog}} * 100\% \quad (1)$$

$$\varepsilon_{rec} = \left(\varepsilon_{prog}\right) + \left(\varepsilon_{th}\right) - \varepsilon_{irr} \quad (2)$$

$$R_f = \frac{\varepsilon_{new}}{\varepsilon_{prog}} * 100\% \quad (3)$$

$$R = R_r * R_f \quad (4)$$

Here, R_r is the structure recovery ratio linked to the level of ε_{rec} and ε_{prog}, if ε_{rec}= ε_{prog}, this means structure recovered to its 100 %. Similarly, R_f is the shape fixity ratio represents fixity of the programmed structure after unloading, where due to elastic effects the programmed structure slip-back to a new position or new strain (ε_{new}). If $\varepsilon_{new} = \varepsilon_{prog}$ it implies a 100 % shape fixity ratio of this structure. Finally, R of Eq.4 is a comprehensive factor to evaluate the overall shape memory performance while multiplying the R_r and R_f sometimes referred to as the shape memory index (SMI) [44].

Further work in this area will build upon the design of these finger-inspired cylinder structures leading to more complex structures such as prehensile hands for soft robotics. These complex lattices will be difficult to simulate in terms of the shape memory action given the extreme

complexity of the lattices; however, simulations will be necessary in order to optimally design the spatial variation in more ambitious and complex forms depending on application requirements. Future work will include simulation and verifying models for these current cylinder models as a first foundational step. Additionally, we will repeat these experiments using materials we have developed for AM that allow for the memorization of multiple shapes with multiple switch temperatures.

Acknowledgements

Funding for this work was provided by National Science Foundation (NSF) under grant number CMMI 2227573. We also acknowledge support from the Mr. and Mrs. Macintosh Chair III in Engineering at the University of Texas at El Paso.

References

1. Quanjin M, Rejab MRM, Idris MS, Kumar NM, Abdullah MH, Reddy GR. Recent 3D and 4D intelligent printing technologies: A comparative review and future perspective. Procedia Comput Sci. 2020;167: 1210–1219.

2. Arif ZU, Khalid MY, Zolfagharian A, Bodaghi M. 4D bioprinting of smart polymers for biomedical applications: recent progress, challenges, and future perspectives. React Funct Polym. 2022;179: 105374.

3. Zhao W, Liu L, Zhang F, Leng J, Liu Y. Shape memory polymers and their composites in biomedical applications. Mater Sci Eng C Mater Biol Appl. 2019;97: 864–883.

4. Kuang X, Roach DJ, Wu J, Hamel CM, Ding Z, Wang T, et al. Advances in 4D printing: Materials and applications. Adv Funct Mater. 2019;29: 1805290.

5. Dayyoub T, Maksimkin AV, Filippova OV, Tcherdyntsev VV, Telyshev DV. Shape Memory Polymers as Smart Materials: A Review. Polymers . 2022;14. doi:10.3390/polym14173511

6. Hassan H, Hallez H, Thielemans W, Vandeginste V. A review of electro-active shape memory polymer composites: Materials engineering strategies for shape memory enhancement. Eur Polym J. 2024;208: 112861.

7. Bahl S, Nagar H, Singh I, Sehgal S. Smart materials types, properties and applications: A review. Materials Today: Proceedings. 2020;28: 1302–1306.

8. Liu Y, Du H, Liu L, Leng J. Shape memory polymers and their composites in aerospace applications: a review. Smart Mater Struct. 2014;23: 023001.

9. Jiang HY, Kelch S, Lendlein A. Polymers move in response to light. Adv Mater. 2006;18: 1471–1475.

10. Lendlein A, Jiang H, Jünger O, Langer R. Light-induced shape-memory polymers. Nature. 2005;434: 879–882.

11. Enferadi A, Baniassadi M, Baghani M. Innovative multiphysics approach for designing high-performance thermo-responsive shape memory polymer microvalve. European Journal of Mechanics - A/Solids. 2024;103: 105174.

12. Meng H, Mohamadian H, Stubblefield M, Jerro D, Ibekwe S, Pang S-S, et al. Various shape memory effects of stimuli-responsive shape memory polymers. Smart Mater Struct. 2013;22: 093001.

13. Yang J, Zheng Y, Sheng L, Chen H, Zhao L, Yu W, et al. Water Induced Shape Memory and Healing Effects by Introducing Carboxymethyl Cellulose Sodium into Poly(vinyl alcohol). Ind Eng Chem Res. 2018;57: 15046–15053.

14. Nadgorny M, Xiao Z, Chen C, Connal LA. Three-Dimensional Printing of pH-Responsive and Functional Polymers on an Affordable Desktop Printer. ACS Appl Mater Interfaces. 2016;8: 28946–28954.

15. Shie M-Y, Shen Y-F, Astuti SD, Lee AK-X, Lin S-H, Dwijaksara NLB, et al. Review of Polymeric Materials in 4D Printing Biomedical Applications. Polymers . 2019;11. doi:10.3390/polym11111864

16. Khaliq MH, Gomes R, Fernandes C, Nóbrega JM, Ferrás LL. On the Use of High Viscosity Polymers in the Fused Filament Fabrication Process. Rapid Prototyping Journal. 2017;23. doi:10.1108/RPJ-02-2016-0027

17. Xiao R, Yakacki CM, Guo J, Frick CP, Nguyen TD. A predictive parameter for the shape memory behavior of thermoplastic polymers. J Polym Sci B Polym Phys. 2016;54: 1405– 1414.

18. Yang WG, Lu H, Huang WM, Qi HJ, Wu XL, Sun KY. Advanced Shape Memory Technology to Reshape Product Design, Manufacturing and Recycling. Polymers . 2014;6: 2287–2308.

19. Melly SK, Liu L, Liu Y, Leng J. Active composites based on shape memory polymers: overview, fabrication methods, applications, and future prospects. J Mater Sci. 2020;55: 10975–11051.

20. Xia Y, He Y, Zhang F, Liu Y, Leng J. A Review of Shape Memory Polymers and Composites: Mechanisms, Materials, and Applications. Adv Mater. 2021;33: e2000713.

21. Jenett B, Cameron C, Tourlomousis F, Rubio AP, Ochalek M, Gershenfeld N. Discretely assembled mechanical metamaterials. Sci Adv. 2020;6. doi:10.1126/sciadv.abc9943

22. Jebellat E, Baniassadi M, Moshki A, Wang K, Baghani M. Numerical investigation of smart auxetic three-dimensional meta-structures based on shape memory polymers via topology optimization. J Intell Mater Syst Struct. 2020;31: 1838–1852.

23. Santo L, Quadrini F, Bellisario D. Shape memory composite antennas for space applications. IOP Conference Series Materials Science and Engineering. 2016;161: 012066.

24. Delaey J, Dubruel P, Van Vlierberghe S. Shape-memory polymers for biomedical applications. Adv Funct Mater. 2020;30: 1909047.

25. Lendlein A, Behl M, Hiebl B, Wischke C. Shape-memory polymers as a technology platform for biomedical applications. Expert Rev Med Devices. 2010;7: 357–379.

26. González-Martínez E, Moran-Mirabal J. Shrinking Devices: Shape-Memory Polymer Fabrication of Micro-and Nanostructured Electrodes. Chemphyschem. 2024;25: e202300535.

27. Pantoja M, Jian P-Z, Cakmak M, Cavicchi KA. Shape memory properties of polystyrene-*block*-poly(ethylene-*co*-butylene)-*block*-polystyrene (SEBS) ABA triblock copolymer thermoplastic elastomers. ACS Appl Polym Mater. 2019;1: 414–424.

28. Mehrpouya M, Vahabi H, Janbaz S, Darafsheh A, Mazur TR, Ramakrishna S. 4D printing of shape memory polylactic acid (PLA). Polymer . 2021;230: 124080.

29. Bermudez D, Quiñonez PA, Vasquez EJ, Carrete IA, Word TJ, Roberson DA. A Comparison of the physical properties of two commercial 3D printing PLA grades. Virtual Phys Prototyp. 2021;16: 178–195.

30. Taib N-AAB, Rahman MR, Huda D, Kuok KK, Hamdan S, Bakri MKB, et al. A review on poly lactic acid (PLA) as a biodegradable polymer. Polym Bull. 2023;80: 1179–1213.

31. Nagarajan V, Mohanty AK, Misra M. Perspective on Polylactic Acid (PLA) based Sustainable Materials for Durable Applications: Focus on Toughness and Heat Resistance. ACS Sustainable Chem Eng. 2016;4: 2899–2916.

32. Álvarez-Trejo A, Cuan-Urquizo E, Bhate D, Roman-Flores A. Mechanical metamaterials with topologies based on curved elements: An overview of design, additive manufacturing and mechanical properties. Mater Des. 2023;233: 112190.

33. Jiao P, Mueller J, Raney JR, Zheng XR, Alavi AH. Mechanical metamaterials and beyond. Nat Commun. 2023;14: 6004.

34. Yu X, Zhou J, Liang H, Jiang Z, Wu L. Mechanical metamaterials associated with stiffness, rigidity and compressibility: A brief review. Prog Mater Sci. 2018;94: 114–173.

35. Kumar N, Sonika, Suthar B, Rostami A. Novel optical behaviors of metamaterial and polymer-based ternary photonic crystal with lossless and lossy features. Opt Commun. 2023;529: 129073.

36. Bertoldi K, Vitelli V, Christensen J, van Hecke M. Flexible mechanical metamaterials. Nature Reviews Materials. 2017;2: 1–11.

37. Kolken HMA, Zadpoor AA. Auxetic mechanical metamaterials. RSC Adv. 2017;7: 5111–5129.

38. Zhao W, Yue C, Liu L, Leng J, Liu Y. Mechanical behavior analyses of 4D printed metamaterials structures with excellent energy absorption ability. Compos Struct. 2023;304: 116360.

39. Sabouni-Zawadzka A. Atcive control of smart tensegrity structures. Archives of Civil Engineering. 2014; 517–534.

40. Al Sabouni-Zawadzka A, Gilewski W. Soft and Stiff Simplex Tensegrity Lattices as Extreme Smart Metamaterials. Materials . 2019;12. doi:10.3390/ma12010187

41. Ming G, Liu L, Liu Y, Leng J. Space deployable parabolic reflector based on shape memory polymer composites. Compos Struct. 2023;304: 116327.

42. Dong Y, Chen K, Liu H, Li J, Liang Z, Kan Q. Adjustable mechanical performances of 4D- printed shape memory lattice structures. Compos Struct. 2024;334: 117971.

43. Pei E, Loh GH. Technological considerations for 4D printing: an overview. Progress in Additive Manufacturing. 2018;3: 95–107.

44. Quiñonez PA, Ugarte-Sanchez L, Bermudez D, Chinolla P, Dueck R, Cavender-Word TJ, et al. Design of Shape Memory Thermoplastic Material Systems for FDM-Type Additive Manufacturing. Materials . 2021;14. doi:10.3390/ma14154254

45. Belloni V, Ravanelli R, Nascetti A, Di Rita M, Mattei D, Crespi M. py2DIC: A New Free and Open Source Software for Displacement and Strain Measurements in the Field of Experimental Mechanics. Sensors . 2019;19. doi:10.3390/s19183832

46. Akbar, I.; Mansori, M.E. 4D Printing of Lattice Structures to Test Their Behavior by Repetitive Shape Processing Cycles. *Materials Today Communications* 2024, *39*, 109147, doi:10.1016/j.mtcomm.2024.109